ALEPH 95-051
PHYSIC 95-047
2 May 1995

Update of the search for excited charged leptons, decaying radiatively

T. Medcalf and J. H. von Wimmersperg-Toeller
Royal Holloway

May 2, 1995

1 Introduction

This ALEPH Note updates the results in the previous ALEPH papers [1, 2, 3]. The analyses have been significantly improved by better kinematical and channel selection and in addition, problem areas which were previously not statistically significant have been investigated thoroughly.

Excited lepton states are expected in models in which leptons are composite particles. At LEP, excited leptons ℓ^*, can be produced in pairs, i.e. $Z \rightarrow \ell^*\overline{\ell^*}$, due to normal gauge couplings or singly, i.e. $Z \rightarrow \ell^*\ell$, due to a radiative transition between the normal and the excited lepton. Here l stands for the ordinary lepton - electron, muon, tau or neutrino (excited neutrino production is not considered here). One of the decay modes of an excited lepton is to an ordinary lepton and a photon. Excited leptons have until recently, been searched for through their radiative decay modes because leptonic radiative decays are theoretically favoured. At LEP energies, another possibility is the decay to a lepton and a weak boson [4] e.g. $e^* \rightarrow eZ$ or $e^* \rightarrow \nu_e W$. However weak decays will not be considered in this note and excited lepton decay henceforth refers to radiative decay.

For pair production of excited charged leptons, the tree-level cross sections are as for the standard leptons given in "Z Physics at LEP" [5].

Single production consists of two processes - the s-channel process in which the Z propagator diagram is dominant and the t-channel process in which the photon propagator diagram dominates, available only for electrons in the final state. In pair production, if the excited lepton is assumed to couple to the Z boson via Standard Model couplings, pair production will readily occur if the mass of the excited lepton is less than $m_Z/2$. It is assumed that any ℓ^* decays immediately through $\ell^* \rightarrow l\gamma$.

Although there are several models for excited lepton production, the formulation of Hagiwara et al. [6] is followed throughout this paper. The single production of an excited lepton ℓ^* depends on the strength of its coupling - for single production in the s-channel on $c_{Z\ell^*\ell}$ and for single production in the t-channel on $c_{\gamma e^* e}$. The probability of observing an excited lepton of mass between $m_Z/2$ and m_Z depends essentially on the coupling. The general form of the effective lagrangian for the $\ell^*\ell V$ transitions is written

$$\mathcal{L}_{\text{eff}} = \sum_{V=\gamma,Z,W} \frac{e}{\Lambda} \bar{L}\sigma^{\mu\nu}(c_{VL\ell} - d_{VL\ell}\gamma^5)\ell\partial_\mu V_\nu + \text{h.c.}$$

To high accuracy the $g-2$ measurements imply $|c| = |d|$ for the couplings and the absence of electric dipole moment requires c and d to be relatively real. For the analyses described here, $V = \gamma, \mathrm{Z}$ and the couplings are expressed in terms of Λ and c.

2 Analysis Event Samples

For each excited lepton search, data, background and signal event samples were selected as follows : the data sample used all events from 1990, 1991, 1992 and 1993 corresponding to approximately 73.5pb^{-1}, that is, 1,800,000 hadronic events.

The background was generated to be equivalent to approximately 10 times the amount of real data i.e. 735pb^{-1}, using physics generators modified to pass on to the detector simulation only events which passed loose kinematical cuts. For the $e^+e^- \to e^+e^-\gamma$ process, the first order QED generator BABAMC [7, 8] was used , while TEEGG7 [9] was used for the process $e^+e^- \to e^{\pm}\gamma$ ($\mu^+\mu^-$ and $\tau^+\tau^-$ events contribute nothing to this channel and the very small contribution from conversions in 2-γ final states is included). For the reactions $e^+e^- \to \mu^+\mu^-\gamma$ and $e^+e^- \to \tau^+\tau^-\gamma$, KORALZ [10] was used. This generator contains some higher order corrections and is expected to describe QED fairly well, although second order final state radiation is missing. For $q\bar{q}$ background, approximately two times the amount of real data was used at the peak centre of mass energy.

To see how effective the cuts are and to calculate the detection efficiencies for each channel, 2000 events of the signal Monte Carlo at each mass in 5 GeV/c^2 step intervals (starting at a mass of 10 GeV/c^2) were generated and passed through the 1990, 1991, 1992 and 1993 detector simulation, in the appropriate proportions. These signal generators do not contain radiative corrections, but the effect of these corrections on the cross-sections has been taken into account in the determination of limits, and their effect on mass-resolutions has been estimated using some signals generated with initial-state corrections up to second order.

3 Data Selection

3.1 Run and event selection

The event selection was made for all PERF or MAYB runs which satisfied the standard searches run selection. For those runs for which the luminosity was unavailable, the Monte Carlo was normalised to the number of hadronic events.

3.2 Charged track and photon definitions

The Aleph energy flow algorithms were used [2] and all subsequent analysis conducted with energy flow objects, both charged and neutral. To be counted as 'good', tracks or photons must form an angle with the beam direction of at least 18.2°. Only events with one, two or four charged tracks, with a zero sum of charges in the latter two cases, were accepted for further analyses.

Photons are identified from clusters of electromagnetic energy, by shower estimators within the energy flow package and required to have energy greater than 10 GeV.

4 Search for $e^+e^- \to \gamma \to e^*e$

In high energy e^+e^- collisions, a virtual photon emitted by one of the incoming particles can be elastically scattered by the other. This quasi-real Compton scattering is the main background to the production of an e^* in the t-channel, The 'spectator' electron which radiates the photon continues at a low angle and thus remains undetected. The other electron and the photon scatter off each other and are in general detected in the central part of the detector, both particles being in a plane containing the beam direction. In earlier analyses of this channel, more stringent angular acceptance cuts were made on both electron and photon, but these limit the e^*-mass range discoverable at the low end, due to relativistic collimation in the signal, and do not improve the high mass limit.

In this process, the final state is characterized by a single detected charged track and one energetic photon, which are the products of the e^* decay for the signal. The visible energy, the sum of the track momentum and of the photon energy, is larger than the beam energy. Due to the imbalance in the initial state between the photon and the beam momenta, the event is boosted in the direction of the beam of the same sign as the detected electron or positron. In general, the overconstrained kinematics of this process makes the associated events rather easy to separate from any background.

To select the events associated to the quasi-real Compton scattering diagram, only two cuts were applied initially. The planarity of the final state was ensured by asking that the angle between the photon direction and the normal to the plane defined by the charged track and the beam direction be less that 90.5° but larger than 89.5°. Compared to [?], this cut has been tightened (from $90 \pm 1o$), because this definition of the angle used to test planarity is more effective than the one previous used, involving the cross product of vectors (track and photon) that are often nearly antiparallel. Next the total final state energy, that is, the sum of the measured photon energy, the track momentum of the visible electron and the energy of the undetected electron, calculated using the measured polar angles of the photon and the detected electron, is required to be greater than 92.5 % of the total centre-of-mass energy, i.e.

$$P_e + E_\gamma + E_{\rm cms}\ \beta/(1+\beta) > 0.925 E_{\rm cms}$$

where $\beta = -Q_e \frac{\sin(\theta_e+\theta_\gamma)}{\sin\theta_e+\sin\theta_\gamma}$, and Q_e is the charge of the detected lepton (the minus sign arises because the electron beam goes in the Aleph +z-direction, by convention).

Events are also rejected if the track does not satisfy electron identification criteria [2]. At this point in the analysis, 4600 events remain. However, a large number of events is found for which the angle between the photon and the charged track is $\sim 180°$. These collinear events arise from large angle Bhabhas where one of the final state electrons has too little momentum to reach (or be reconstructed in) the TPC. Visual scanning of these events confirmed this hypothesis and the distribution of number of ITC hits versus the opening angle between the $e\gamma$ final state particles clearly shows this background: it was removed by requiring less than 13 ITC hits (but at least 4 hits) when the opening angle between the visible particles is larger than 175°.

The final data sample of $e\gamma$ events consists of 1892 events, only 1782 of which have positive β-factors. $\beta < 0$ implies that the observed track has a z-cpt oppositely directed to that of the beam particle of the same charge, and can be assumed to come from the small s-channel contribution to the background. 1777.6 background events are predicted,

the agreement being well within the statistical error. The event breakdown is shown in table 1.

Table 1: Breakdown of events through the t-channel e* analysis.

Number of events	*Data*	*Monte Carlo*
1-track, 1-photon events	8484	3512.9
after planarity cut	5859	2166.0
after total energy cut	4759	2041.6
after QEIDO cut	4348	1959.8
after ITC cut	1892	1797.3
after $\beta > 0$ cut	1782	1777.6

5 Event Selection for Single and Pair Production

5.1 Kinematical Selection

Initially all events with two and four charged tracks were required to satisfy three kinematical cuts and selected according to the number of hard (> 10 GeV) photons. The photon energy spectrum in radiative leptonic Z decays falls rapidly with increasing energy (e.g. unbroken line in fig. 1.a). As can be seen from this figure, the photon energy spectrum originating from single production excited lepton decay has a lower limit of about 10 GeV for an excited lepton of mass 45 GeV/c^2 and increases with the mass (fig. 1.b). For pair production, the photon energy increases with the mass of the excited lepton. To remove as much radiative background as possible, the photon energy is cut at 10 GeV.

The majority of background consists of two-track e^+e^-, $\mu^+\mu^-$ and $\tau^+\tau^-$ events. Photon emission mainly occurs at low energy so that the photon is usually very close to the track and the two charged tracks are almost back-to-back, i.e. the angle between the tracks is $\sim$ 180°. Hence only those events are selected where the photon is more than 25° from any track, and the track acollinearity is smaller than 170° but greater than 10°. The last part of the cut is used to remove photon conversions since in general the tracks arising from a conversion are very close together. The acollinearity cut is not applied to the four track topology.

5.2 Selection of $e^+e^- \rightarrow e^*e$ and $e^*\overline{e^*}$ candidates

In an event in which the charged tracks are all electrons, essentially all the track-energy should appear in the electromagnetic calorimeter. The total electromagnetic energy measured minus the photon energy was required to be larger than 75 % of the total available energy once the photon(s) are radiated,

$$E1_{\mathrm{nor}} = \frac{E_{em} - \sum E_\gamma}{E_{\mathrm{cms}} - \sum E_\gamma} > 0.75$$

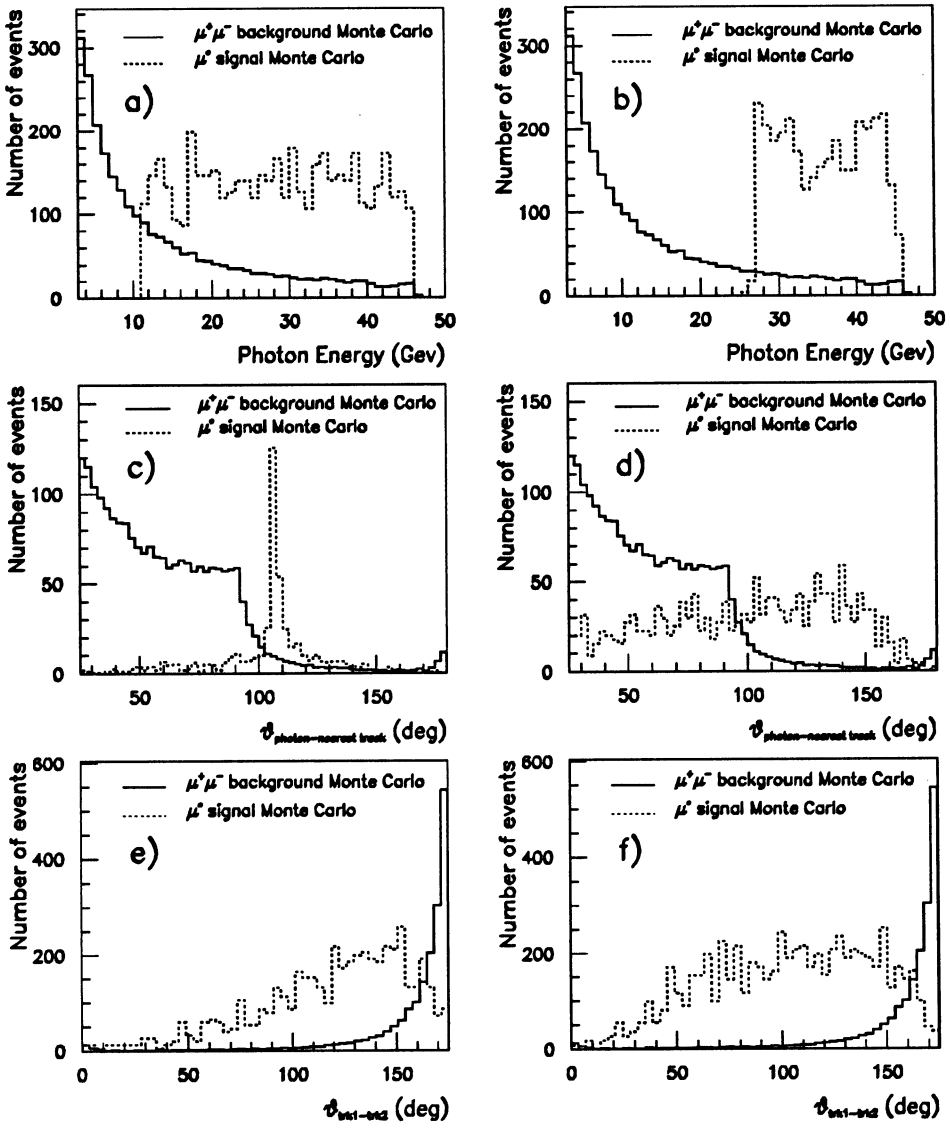

Figure 1: Kinematics of excited lepton single production. Photon energy spectrum (for coupling $C_{Z\mu^*\mu}/\Lambda$ chosen to optimize the displays) plus background, for a) 45 GeV/c^2 excited muon ($C_{Z\mu^*\mu}/\Lambda = 10^{-2}$), b) 70 GeV/$c^2$ excited muon (10^{-3}). The angle between the photon and nearest charged track for c) 45 GeV/c^2 excited muon (10^{-3}), d) 70 GeV/c^2 excited muon (5×10^{-3}). The angle between the charged tracks for e) 45 GeV/c^2 excited muon (10^{-2}), f) 70 GeV/c^2 excited muon (2×10^{-2}).

This requirement alone isolates, with a high efficiency, final states where electromagnetic energy dominates. Finally, in order to check the electron identification, at least one charged track must be positively identified from shower estimators similar to those used for photons [2], to remove a small number of strongly radiative non-electron events.

The final sample consists of 1451 $e^+e^-\gamma$ events compared to 1617.3 predicted from the hard radiative electroweak reaction $e^+e^- \to e^+e^-\gamma$ as seen in table 2. This disagreement will be discussed later in section 8. For the $e^*\overline{e^*}$ search, 6 $e^+e^-\gamma\gamma$ events were seen compared to 2.2 events predicted by BHAB01. The failure of BHAB01 to fully describe the $e^+e^- \to e^+e^-n\gamma$ process will be discussed in section 7.

		Monte Carlo		
Analysis stage	DATA	$e^+e^-\gamma$	$\mu^+\mu^-\gamma$	$\tau^+\tau^-\gamma$
2-track events	12887	5674.7	3823.1	2440.6
After acollinearity	5560	1941.6	1179.6	765.4
1 photon above 10 GeV	3246	1771.7	979.2	512.1
After $E1_{nor} > 0.75$	1468	1619.6	0.0	2.0
After QEIDO	1451	1617.3	0.0	1.5

Table 2: Breakdown of events through the $e^+e^- \longrightarrow e^+e^-\gamma$ analysis for the excited electron search. A match between data and Monte Carlo should be expected after the acollinearity cut since the Monte Carlo has been generated using loose kinematical cuts.

Signal efficiencies are of the order of 60 % and above, in this channel, except at very high m_{e^*}, see fig. 2b.

5.3 Selection of $e^+e^- \to \mu^*\mu$ and $\mu^*\overline{\mu^*}$ candidates

Initially, only those events were selected where the total visible electromagnetic energy, except that corresponding to the photon, is small. For this, the total ECAL energy measured minus the photon energy was required to be smaller than 10 % of the total centre-of-mass energy,

$$E2_{\rm nor} = \frac{E_{em} - \sum E_\gamma}{E_{cms}} < 0.1$$

This removes all the Bhabha events and a large fraction of the $\tau^+\tau^-$ events. A second cut removes essentially all remaining background, by selecting those events where the sum of the charged particle momenta and of the photon energy is larger than 80 % of the total centre-of-mass energy, i.e.

$$E3_{\rm nor} = \frac{\sum p + \sum E_\gamma}{E_{cms}} > 0.8$$

In order to check the muon identification, at least one track must be positively identified by the muon-chamber hits and/or a characteristic pattern in the last few planes of the hadron calorimeter.

The final sample consists of 913 $\mu\mu\gamma$ events compared to 946.8 predicted from the hard radiative electroweak reaction $e^+e^- \to \mu^+\mu^-\gamma$ as seen in table 3. For the $\mu^*\overline{\mu^*}$ search, 10

Analysis stage	DATA	Monte Carlo		
		$\mu^+\mu^-\gamma$	$e^+e^-\gamma$	$\tau^+\tau^-\gamma$
2-track events	12887	2843.3	3902.2	1927.2
After acollinearity	5560	1179.6	1941.6	765.4
1 Photon above 10 GeV	3246	979.2	1771.7	512.1
After $E2_{nor} < 0.1$	1158	976.6	7.6	172.0
After $E3_{nor} > 0.80$	953	969.6	7.3	9.3
After QMUIDO	913	946.8	0.0	3.8

Table 3: Breakdown of events through the $e^+e^- \longrightarrow \mu^+\mu^-\gamma$ analysis for the excited muon search. A match between data and Monte Carlo should be expected after the acollinearity cut as the Monte Carlo has been generated using loose kinematical cuts.

$\mu^+\mu^-\gamma\gamma$ events were seen compared to 0.8 events predicted by KORALZ. The failure of KORALZ to fully describe the $e^+e^- \rightarrow \mu^+\mu^- n\gamma$ process will be covered in section 7.

Signal efficiencies are of the order of 60 % and above, in this channel, except at very high m_{μ^*}, see fig. 2c.

5.4 Selection of $e^+e^- \rightarrow \tau^*\tau$ and $\tau^*\overline{\tau^*}$ candidates

For this channel, events with two or four good tracks are considered, and they must have failed the e^+e^--channel cut on the electromagnetic energy. Calculation of the missing mass to the charged tracks is used to distinguish tau-events from events without neutrinos (lower missing mass) and events with additional undetected particles (higher missing mass).

The two track topology is considered first. Events are accepted if the missing mass squared is larger than $500(\text{ GeV}/c^2)^2$ and less than $6500(\text{ GeV}/c^2)^2$. The high cut removes a few mostly higher order Bhabha events. Two more cuts were applied on all events in this topology to remove remaining backgrounds. First, the sum of the charged particle momenta and of the associated electromagnetic cluster energies, E_c, normalized to the available centre-of-mass energy after subtraction of the photon energy, was required to be less than 1.1, i.e.

$$E_{\text{chsum}} = \frac{\sum_{tracks}(p + E_c)}{E_{\text{cms}} - \sum E_\gamma} < 1.1$$

This cut removes the tail of $e^+e^- \rightarrow e^+e^-\gamma$ events where, for example, another hard photon is emitted along the track direction. Secondly, the sum of the charged particle momenta was required to be less than than 80 % of the total available energy (after substraction of the radiated photon energy), i.e.

$$p_{\text{sum}} = \frac{\sum p}{E_{\text{cms}} - \sum E_\gamma} < 0.8$$

This cut mainly removes the remnant contribution from $e^+e^- \rightarrow \mu^+\mu^-\gamma$. In a later section, the τs are reconstructed using a scaling technique (section 6), and events are discarded here if the reconstructed event is severely distorted, as happens when particles

have gone undetected, in directions quite different from those of the tau-decay tracks. At this stage there are 503 data events.

Next four charged track candidates are considered, corresponding to 3-prong decays of one τ only. To remove background from events where the main part of the final state escapes the detection in the forward directions, the missing mass squared is required to be smaller than 6000(GeV/c^2)^2. $e^+e^-\gamma\gamma$ events of the type where one photon converts to an e^+e^- pair are rejected by requiring the missing mass to be greater than 250(GeV/c^2)^2. Tau candidates decaying into three charged particles are selected as triplets of tracks with a total electric charge ± 1 and an invariant mass smaller than 1.6 GeV/c^2 (the pion mass being assumed for the charged particles). If more than one triplet fulfils these conditions, the event is discarded (no such events occur in signal Monte Carlo).

The final sample consists of 691 $\tau^+\tau^-\gamma$ events compared to 659.6 predicted from the hard radiative electroweak reaction $e^+e^- \to \tau^+\tau^-\gamma$ as seen in table 4, together with 21.0 events expected from other backgrounds. For the $\tau^*\overline{\tau^*}$ search, 8 $\tau^+\tau^-\gamma\gamma$ events were seen compared to 0.5 events predicted by KORALZ. Again the failure of KORALZ to fully describe the $e^+e^- \to \tau^+\tau^- n\gamma$ process will be covered in section 7.

Signal efficiencies are of the order of 45 % and above, in this channel, except at very high m_{τ^*}, see fig. 2d.

		Monte Carlo			
Analysis stage	DATA	$\tau^+\tau^-\gamma$	$e^+e^-\gamma$	$\mu^+\mu^-\gamma$	$q\bar{q}\gamma$
2- or 4-track events	15496	2711.8	3952.2	2844.7	380.2
After acollinearity (2 trks only)	8169	1550.0	1991.6	1180.9	355.6
1 photon above 10 GeV	3742	749.8	1794.5	979.7	50.8
$E1_{nor} < 0.75$	2219	745.6	153.6	979.7	50.8
2-track only	1778	510.0	152.6	979.2	17.5
After $\lvert\text{missing mass}\rvert^2$ (2 trks only)	628	473.1	46.9	17.1	17.5
After E_{chsum} (2 tracks only)	562	458.5	9.8	17.1	3.2
After p_{sum} (2 tracks only) and reconstruction	503	454.9	8.0	6.8	1.7
4 tracks only	441	236.5	1.6	0.6	33.3
After $\lvert\text{missing mass}\rvert^2$ (4 trks only)	333	226.7	1.2	0.0	20.0
After inv. mass (1.6 GeV/c^2) and reconstruction	188	204.7	0.8	0.0	4.7
Final sample	691	659.6	8.8	6.8	5.4

Table 4: Breakdown of events through the $e^+e^- \longrightarrow \tau^+\tau^-\gamma$ analysis for the excited tau search. A match between data and Monte Carlo should be expected after the photon isolation cut as the Monte Carlo has been generated using loose kinematical cuts.

6 Invariant mass reconstruction

If the invariant mass of the electron- (or muon-) photon system is calculated directly from the measured momenta, the resolution is of order of 2 GeV/c^2 full width half maximum. However the mass resolution can be improved by using the angular measurements and

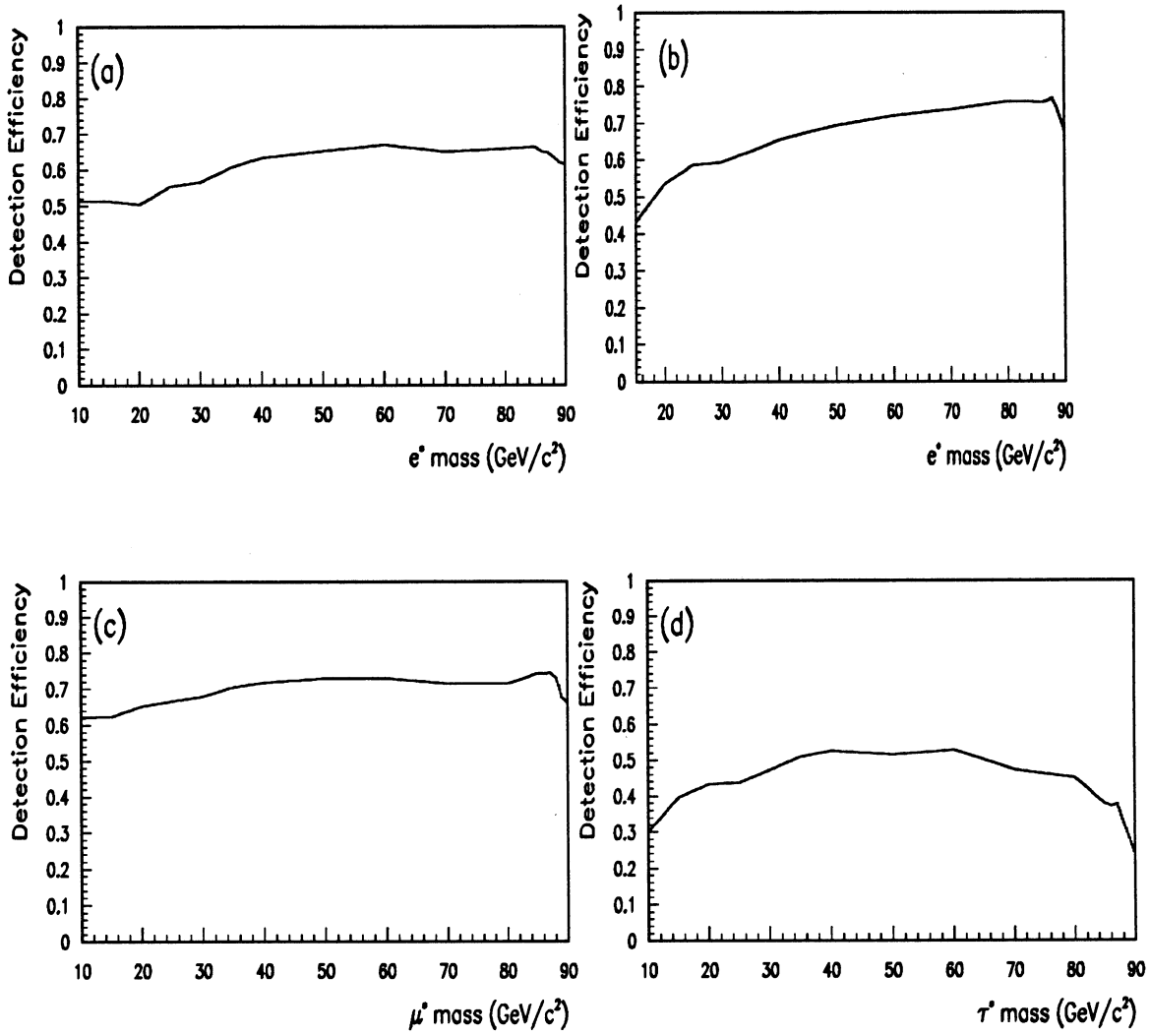

Figure 2: The efficiency of fully simulated signal Monte Carlo for a) e*e s-channel production, b) e*e t-channel production, c) $\mu^*\mu$ production, d) $\tau^*\tau$ production.

rescaling the energies of the charged particles and the photon. Using these re-scaled values, the invariant mass resolutions are about 0.1 GeV/c^2 FWHM for the $e^+e^-\gamma$ (both s and t channels) and the $\mu^+\mu^-\gamma$ channel. In the high mass region above 46 GeV/c^2, all these resolutions are found to be approximately independent of the mass of the particles. For example, the $\mu^*\mu$ resolution is shown in fig. 3, which includes the effects of initial state radiative corrections up to second order.

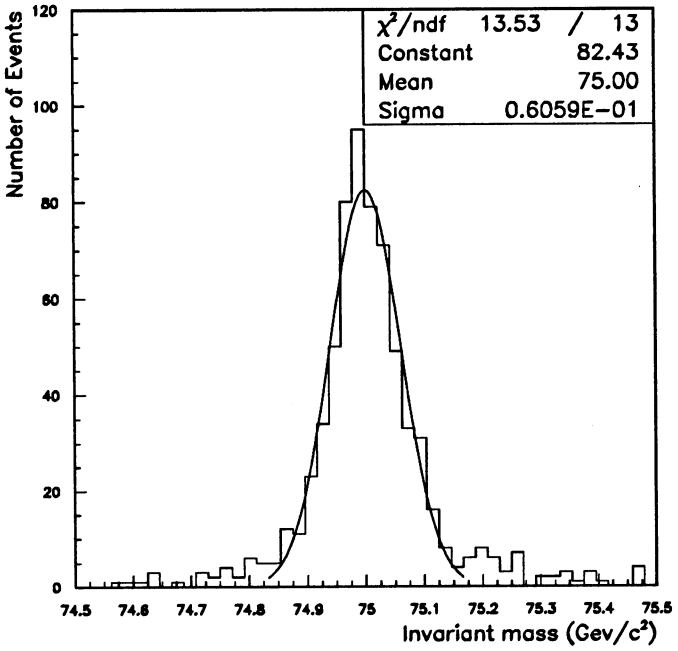

Figure 3: The resolution for the $\mu^*\mu$ channel for an excited muon of mass 75 GeV/c^2.

Reconstructing the invariant mass for the $\tau^+\tau^-\gamma$ channel is slightly more complicated although the general principle is the same. The basic concept is that τs produced at the Z peak are so energetic that all their decay products are relativistically collimated to the extent that the direction of the charged track detected may be taken, with little error, to be the direction of the τ. After re-scaling the momenta of the charged tracks and the energy of the photon, the excited tau resolution is found to be of the order 2.5 GeV/c^2 FWHM.

7 Extraction of Pair Production Mass Limits

In the pair production search, 6 $e^*\overline{e^*}$, 10 $\mu^*\overline{\mu^*}$ and 8 $\tau^*\overline{\tau^*}$ candidate events were found compared to 2.2 $e^+e^-\gamma\gamma$, 0.8 $\mu^+\mu^-\gamma\gamma$ and 0.5 $\tau^+\tau^-\gamma\gamma$ predicted background using the Monte Carlo generators BHAB01 and KORALZ. The BHAB01 generator is only first order and therefore not expected to match the data. The number of predicted events using BHAB01 arise solely from exterior bremsstrahlung. The KORALZ does have some higher orders using exponentiation but this is to provide a more accurate prediction for $\ell^+\ell^-\gamma$ events. Using a second order matrix calculation [11], and making allowance for detection losses not taken into account in [11] the predicted numbers are approximately 10.6, 9.0 and 6.3 for the $e^+e^-\gamma\gamma$, $\mu^+\mu^-\gamma\gamma$ and $\tau^+\tau^-\gamma\gamma$ respectively. This section describes how these events are distinguished from genuine candidates and lower bound limits are set

on the masses of the excited leptons in pair production, using a signal Monte Carlo specifically written for this purpose. This is a simple self-contained Monte Carlo, in that it does not write out simulated data. Everything, from event generation to analysis, is done within the program.

Initially for a given CMS energy and ℓ^* mass, two ℓ^* particles are generated according to the Born electroweak differential cross section for the production of heavy fermions. The two ℓ^*s are produced back to back in the rest frame of the Z. Each ℓ^* then undergoes isotropic decay in its own frame of reference, resulting in a back to back l and γ. Once boosted to the lab frame, fiducial ($|\cos\theta| < 0.95$), good track ($E_{trk} > 2$ GeV) and the same kinematical cuts as in section 5.1 are applied to all final state particles as in the excited lepton analyses above, allowing an acceptance to be calculated. For the τ^* channel, the decayed τ from the τ^* is passed through JETSET so that the τ can be allowed to decay further through its possible hadronic and leptonic decay modes. Generally in the detector, each photon has a 6 % probability of converting to a e^+e^- pair, as it passes through. All photons in the Monte Carlo program at this stage within the angular acceptance and with an energy greater than 1 GeV are allowed to convert with this probability. If a photon converts however, the event is rejected.

Hence the angular acceptance as a function of $\cos\theta$ and $d\sigma/d\Omega$ can be predicted. This was done for all energies and luminosities at which the analyses were carried out.

In order to be compatible with experimental data, additional corrections have to be applied:

- radiative correction: using an approximate first-order initial-state correction in which the photon distribution is assumed to obey Probability $\sim \frac{1}{E_\gamma}$.

- photon finding: photons are detected in the electromagnetic calorimeter; it is possible that the photon path includes areas such as the dead zones between modules in the calorimeter, where detection is not possible; the photon finding correction used was 93 %.

To calculate a mass limit for each pair production channel, the number of events corresponding to all the generated masses and energies are summed and a value for the mass predicted.

From the analyses above, 6 $e^*\overline{e^*}$, 10 $\mu^*\overline{\mu^*}$ and 8 $\tau^*\overline{\tau^*}$ candidate data events are observed. However, if excited leptons are produced in pairs then the pairs should be of the same mass (the τ^*-masses were reconstructed by a amethod similar to that described in section 6). Thus the two pairs of possible invariant mass combinations of the two charged tracks (for taus the triplet is combined into a 'composite' track) and the two photons are formed. The combination giving the smaller difference in invariant masses is then chosen and this difference is compared to the standard deviation in the invariant mass, taken from resolution plots similar to fig. 3. The invariant masses for the candidate events in the three channels together with the 2σ error lines can be seen in fig. 4. Using this method, it is clear from fig. 4 that no events lie within the error lines, for any of the three channels.

Using these error lines to separate background from signal may result in some signal events being lost. Hence the $\ell^*\overline{\ell^*}$ signal Monte Carlo described above was modified to accept events only if the invariant masses of the generated ℓ^* were within the error lines.

In fact no loss from the $e^*\overline{e^*}$ and $\mu^*\overline{\mu^*}$ channels is found while 8% of the generated $\tau^*\overline{\tau^*}$ events are lost. This has been included in the limit calculation.

Since there are zero candidates for all $\ell^*\overline{\ell^*}$ channels, using Poisson statistics, the 95% confidence level is 3 events. Mass limits are determined from the plots given in fig. 5. The mass limits corresponding to the $e^*\overline{e^*}$, $\mu^*\overline{\mu^*}$ and $\tau^*\overline{\tau^*}$ are 46.60 GeV/c^2, 46.60 GeV/c^2 and 46.37 GeV/c^2 for the three channels respectively. This search confirms previous negative results [1] with an increase in statistics. Note that the mass limits are greater than $m_Z/2$ because of the energy scan around the Z peak and only energies at and above twice the mass limit contribute towards the limits.

8 Single Production

The theory of excited leptons has been discussed very briefly in the first section. The formulation of Hagiwara et al. [6] is the one most frequently followed by experimental groups in setting coupling limits.

Using the formula for the Born cross section given in [6] the cross-section σ can be calculated and thus the number of events produced for a given value of Λ (this is taken to be 1000 GeV) as a function of mass, taking into account the integrated luminosity at each energy and the acceptance correction.

Due to the presence of the background, the $c(V\ell^*\ell)/\Lambda$ coupling limit is calculated as a function of ℓ^* mass bin by bin (binning determined by the effective mass resolution (section 6)), given the number of events observed and the background. The invariant mass distributions together with the coupling limit plots are shown in figs 6.a, 8.a, 9.a and 10.a. A chi-squared fit has been performed on the invariant mass data and Monte Carlo curves. All the χ^2's per degree freedom and the χ^2 probabilities for the excited lepton channels (except the e*e s-channel) are good, showing there is agreement between the data and Monte Carlo. The e*e s-channel is rather poor and is discussed below.

The most obvious feature in the e*e channel is the disagreement between the number of observed data and standard model background events. This disagreement arises because the Monte Carlo generator used (BABAMC) to compare with the data is first order in the initial and final state only, i.e. each event contains one radiated photon arising from the initial *or* final state. An investigation into this problem by using a higher order $\mu\mu\gamma$ Monte Carlo (KORALZ), revealed that adding higher orders results in a softening of the photon energy spectrum, when more photons are expected. This softening would itself result in many of the events which would have been accepted to be rejected by the photon energy cut and thus a closer agreement between the Monte Carlo background and the data. From the investigation it was found that this second order effect constitutes approximately a 14% reduction compared to first order, i.e., the number of Monte Carlo events expected is calculated to be 1418.6 compared to 1451 data events, much closer than actually observed. Hence the $ee\gamma$ background curve in fig. 6.a has been normalised to the number of Monte Carlo found from the BABAMC generator and the number of data events actually observed. This re-normalisation does not affect the overall coupling limit. The resulting invariant mass distribution and coupling limit plot are shown in figs 7.a and 7.b.

Considering the current ALEPH coupling limits in comparison to the pre-LEP experiments, ALEPH has greatly improved the sensitivity. Areas in the coupling plot above and

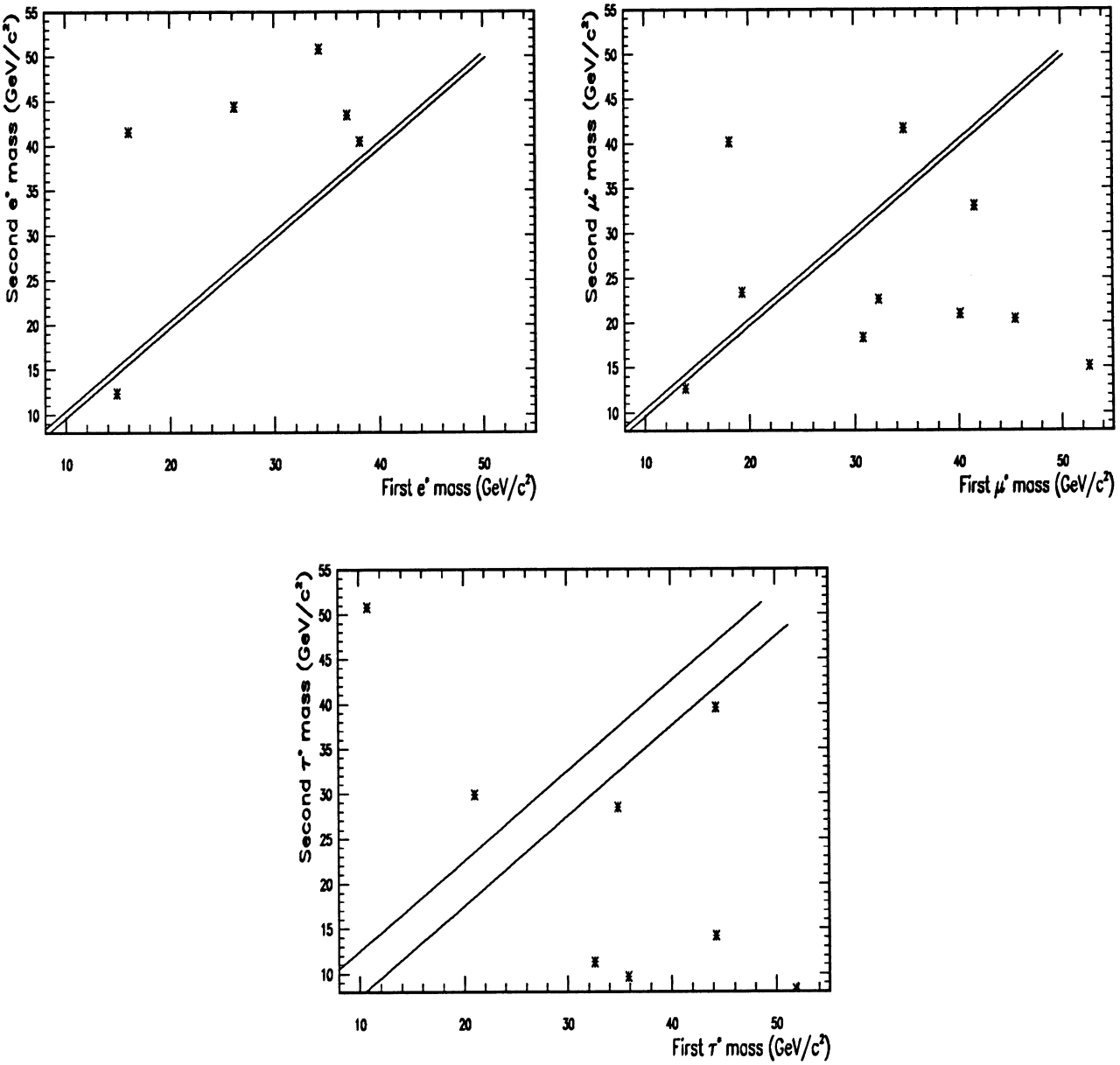

Figure 4: The possible invariant mass combinations of the observed events for $\ell^*\overline{\ell^*}$ production for a) $e^*\overline{e^*}$ (6 entries) b) $\mu^*\overline{\mu^*}$ (10 entries) c) $\tau^*\overline{\tau^*}$ (8 entries).

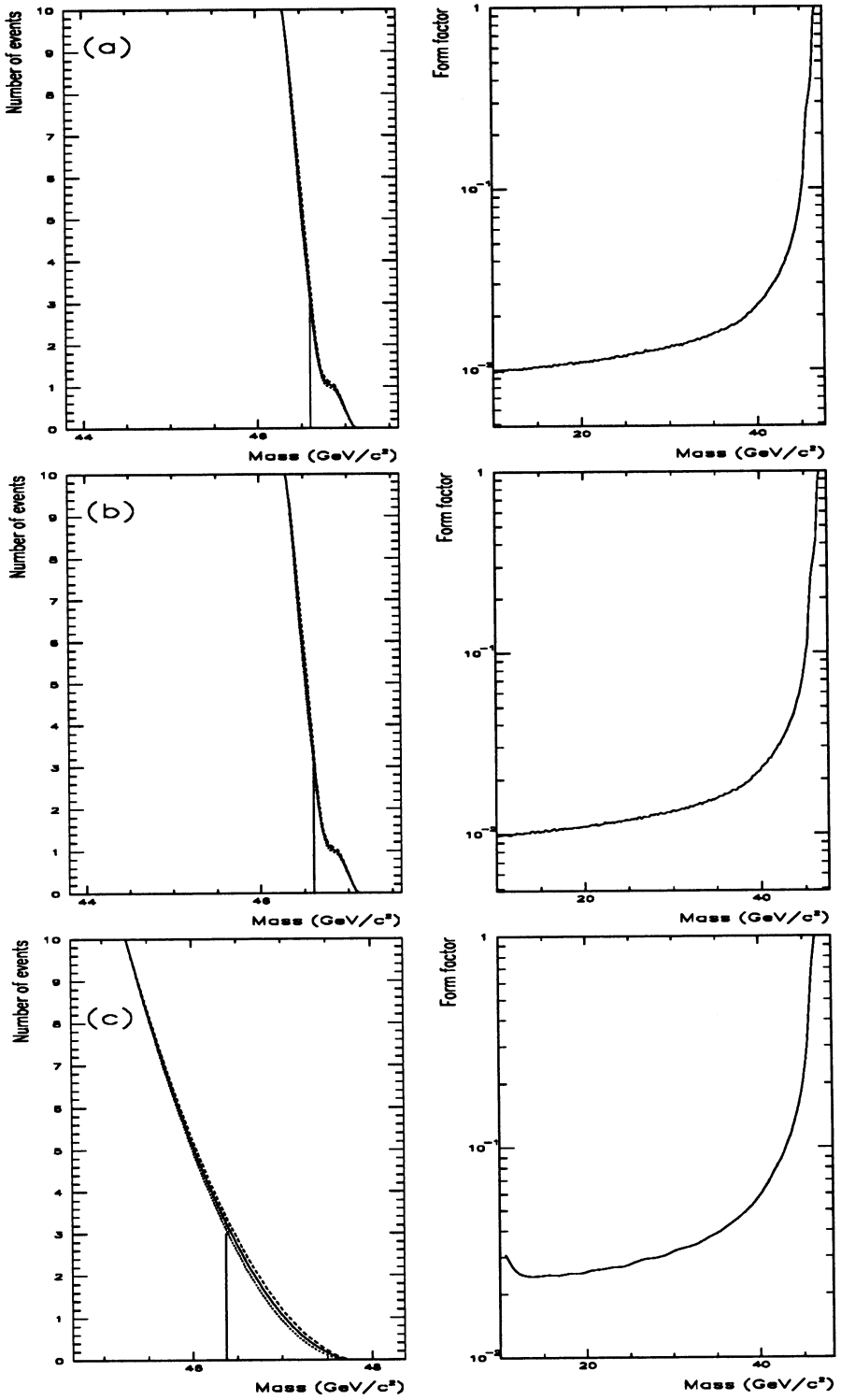

Figure 5: The predicted number of events (left column) and the form-factor limit (right) for $\ell^*\overline{\ell^*}$ production of a) $e^*\overline{e^*}$ b) $\mu^*\overline{\mu^*}$ c) $\tau^*\overline{\tau^*}$. The line shows the mass limit corresponding to zero observed events.

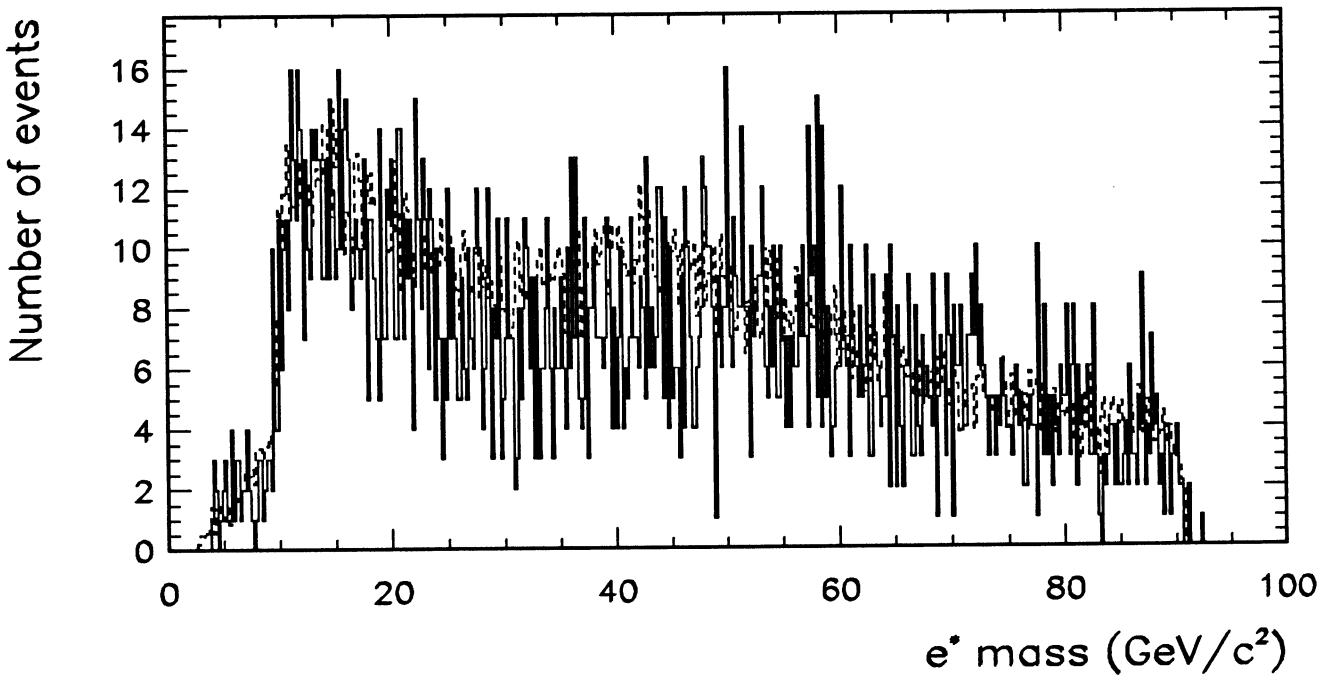

Figure 6: The photon-electron invariant mass distribution (two entries per event).

to the left of the coupling limit curve represent excluded regions where excited lepton production cannot be observed. However, should excited leptons occur, a signal would manifest itself as a large distinct peak above the background in both the invariant mass plot and in the coupling limit curve. The small peaks in the curve are background. These results update previous limits published by ALEPH [1, 2] and are better than current results by other LEP experiments [12, 13, 14, 15]. The HERA detector at DESY has already been running at high energies and therefore has a e*e coupling limit up to at a mass close to 200 GeV/c^2. This coupling limit in the same mass region as LEP is a factor 10 worse [16].

9 Conclusions

Using a data sample corresponding to approximately 1,800,000 hadronic Z decays, the process $e^+e^- \to \ell^+\ell^-\gamma$, (where $\ell = e$, μ or τ) has been studied in order to search for deviations from Standard Model predictions. No such evidence has been found in the searches for e*, μ^*, and τ^*. The existence of excited charged leptons has been excluded for masses up to about 46 GeV/c^2 at 95 % confidence level.

From the measurement of the quasi-real Compton scattering process, $e^+e^- \to e^+e^-\gamma$, a 95 % confidence level upper limit on the γe^*e coupling constant is found to be $c_{\gamma e^*e}/\Lambda < 0.1(\mathrm{TeV}/c^2)^{-1}$ for excited e*e masses up to 90 GeV/c^2. From the measurements of the hard radiative process $e^+e^- \to \ell^*\overline{\ell^*}\gamma$, 95 % confidence level upper limits on the $Z\ell^*\ell$ coupling constant have been calculated to be $c_{\gamma e^*e}/\Lambda < 0.1(\mathrm{TeV}/c^2)^{-1}$ for excited lepton masses around about 50 GeV/c^2 and close to $1(\mathrm{TeV}/c^2)^{-1}$ for masses up to 90 GeV/c^2. These limits on single production significantly extend those published previously by

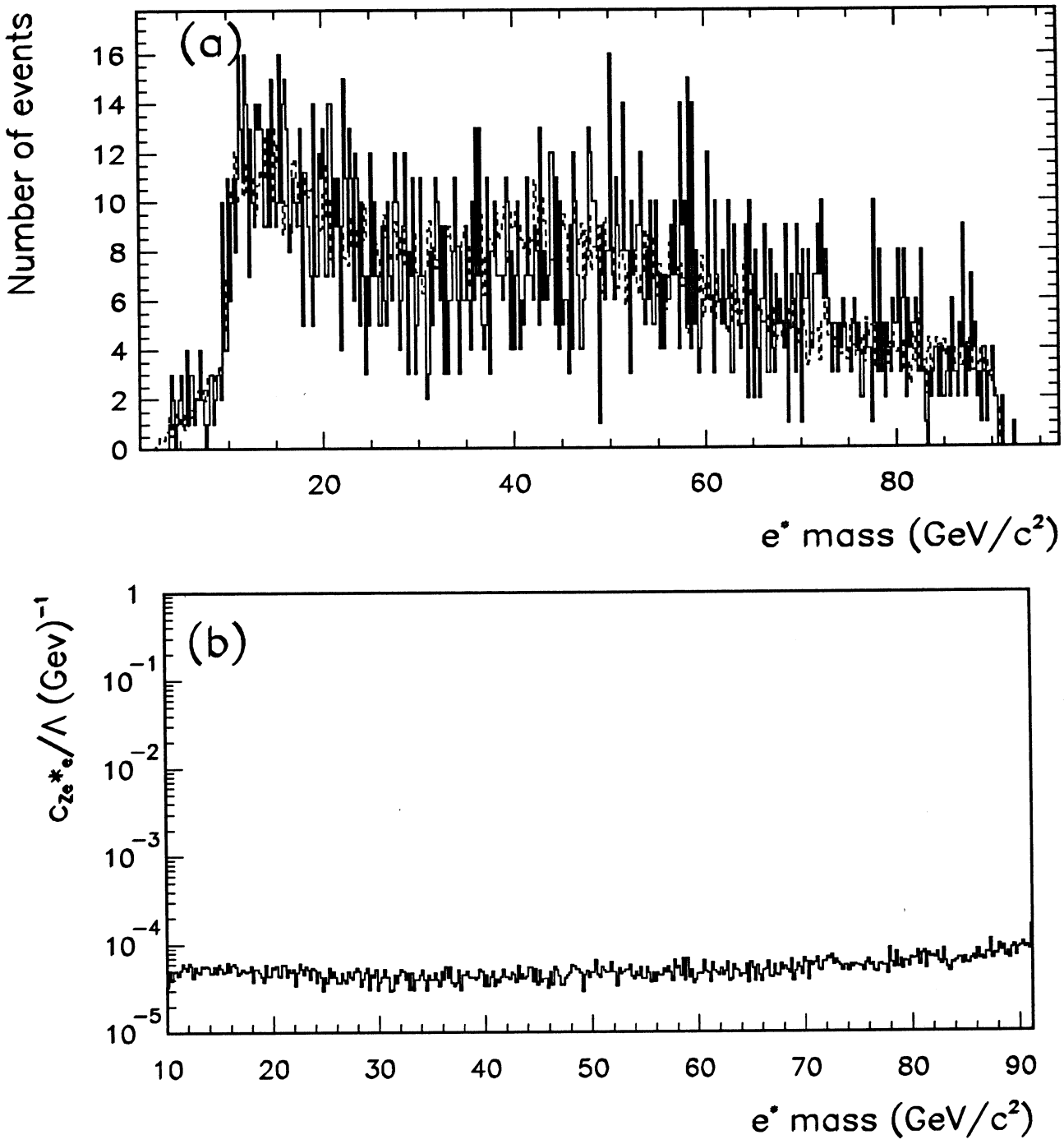

Figure 7: a) The photon-electron invariant mass distribution (two entries per event). The background has been reweighted. (b) The coupling limit c_{Ze^*e}/Λ for the e*e s-channel: region above the line is excluded. (Reweighting the background Monte Carlo has no noticeable effect on the coupling limit curve.)

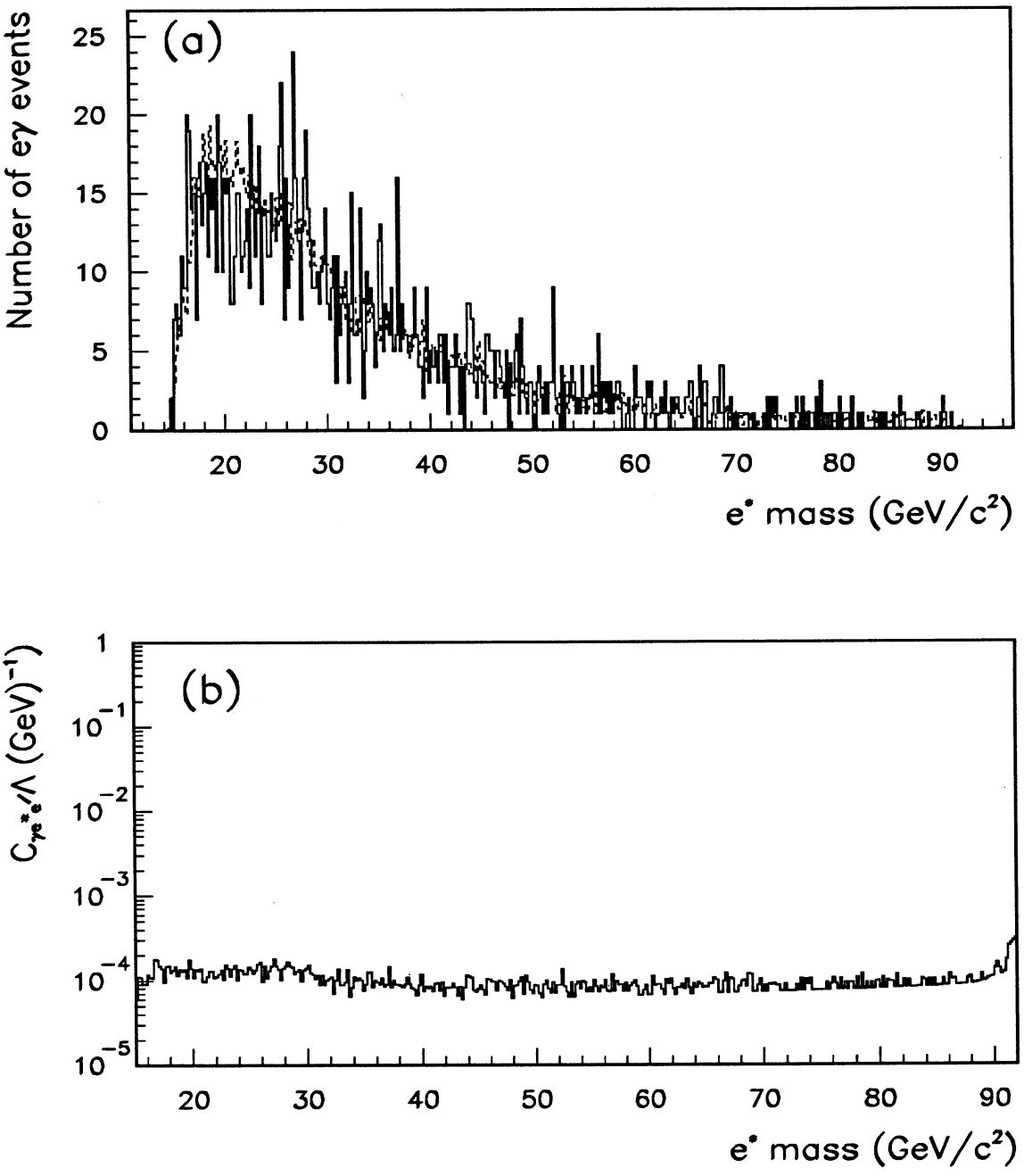

Figure 8: a) The photon-electron invariant mass distribution b) The coupling limit $c_{\gamma e^* e}/\Lambda$ for the e*e t-channel: region above the lin is excluded.

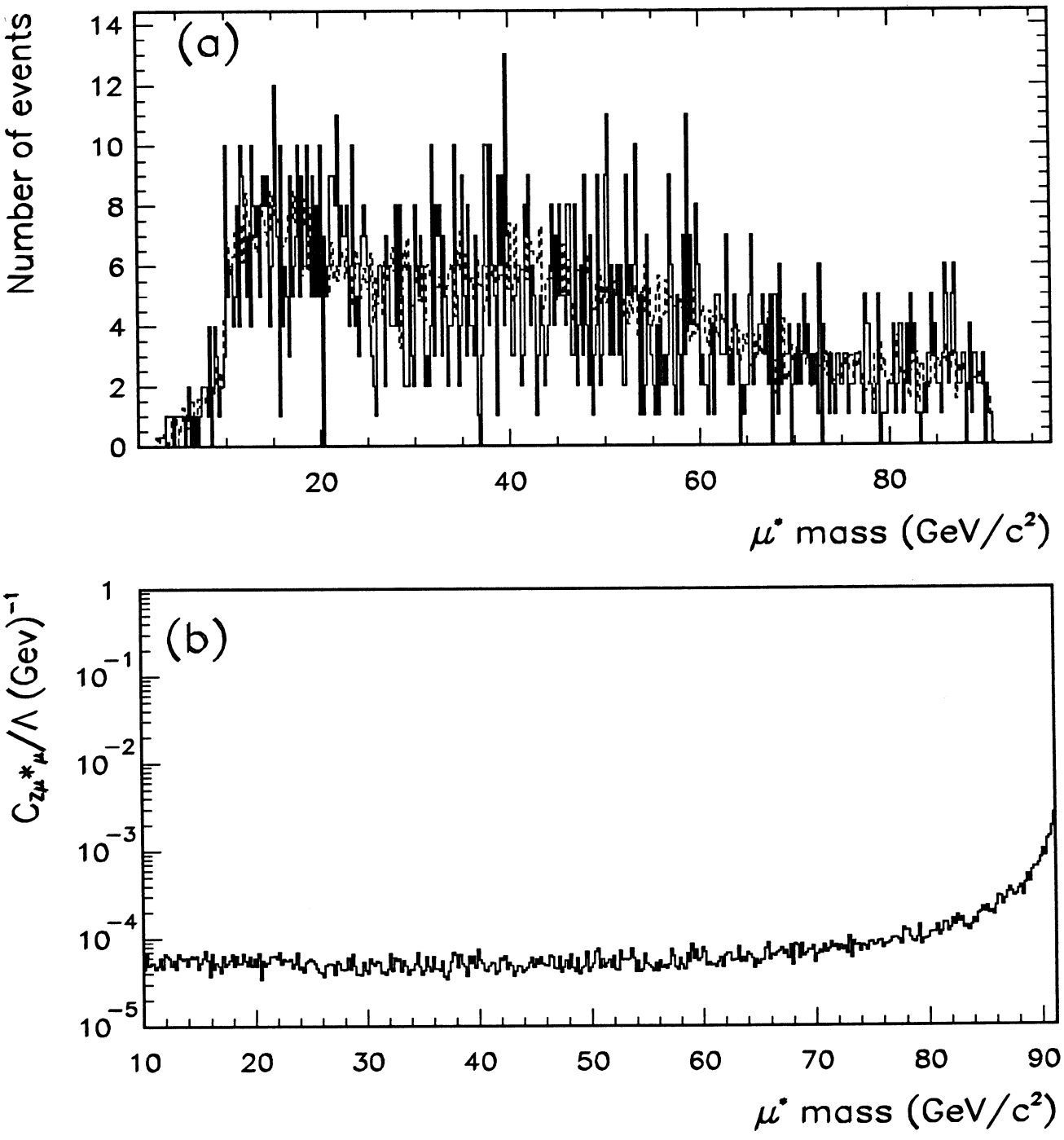

Figure 9: a) The photon-muon invariant mass distribution (two entries per event). b) The coupling limit $c_{Z\mu^*\mu}/\Lambda$: region above the line is excluded.

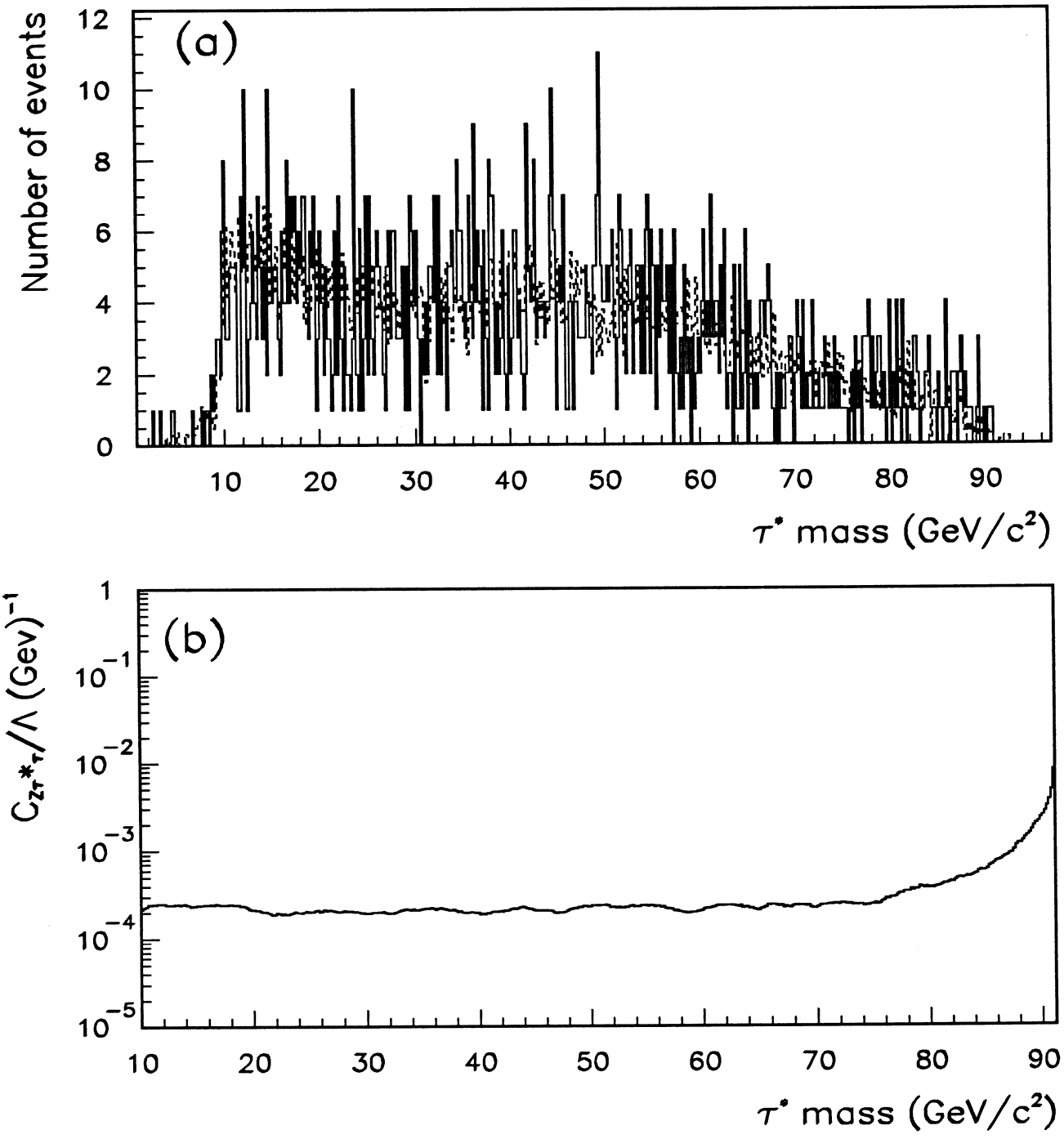

Figure 10: a) The photon-tau invariant mass distribution (two entries per event) b) The coupling limit $c_{Z\tau^*\tau}/\Lambda$: region above the line is excluded.

ALEPH and the other LEP collaborations.

It can be concluded therefore that the measured distributions as well as the rates of the reactions $e^+e^- \to e^+e^-\gamma$, $e^+e^- \to \mu^+\mu^-\gamma$ and $e^+e^- \to \tau^+\tau^-\gamma$, observed in conditions similar to those of a hard radiative process, are in good agreement with Standard Model predictions. For the reaction $e^+e^- \to e^+e^-\gamma$, there is not very good agreement between the data and the Monte Carlo but the disagreement is understood and is associated to lack of higher orders in the Monte Carlo.

References

[1] ALEPH Collaboration, Phys. Lett. **236B** (1990) 4.

[2] ALEPH Collaboration, Phys. Reports, **216** (1992) 1.

[3] ALEPH Collaboration, paper submitted to the Dallas conference (1992)

[4] F. Boudjema *et al.*, DESY 92-116.

[5] Z Physics at LEP Volume 1, CERN 89-08, 12-13.

[6] K. Hagiwara, S. Komamiya and D. Zeppenfeld Z. Phys. **C29** (1985) 115.

[7] M. Bohm, A. Denner and W. Hollik, Nucl. Phys. **B304** (1988) 687.

[8] F. Berends, R. Kleiss and W. Hollik, Nucl. Phys. **B304** (1988) 712.

[9] D. Karlen, Nucl. Phys., B289 (1987) 23.

[10] S. Jadach, B. Ward and Z. Was Comput. Phys. Comm. **66** (1991) 276.

[11] M. Martinez, and R. Miquel, Phys. Lett. B302 (1993) 108.

[12] DELPHI Collaboration, Z. Phys. **53** (1992) 41.

[13] L3 Collaboration, Phys. Lett. **247B** (1990) 199.

[14] L3 Collaboration, Phys. Lett. **250B** (1990) 205.

[15] OPAL Collaboration, Phys. Lett. **244B** (1990) 135.

[16] ZEUS Collaboration, Phys. Lett. **306B** (1993) 173.